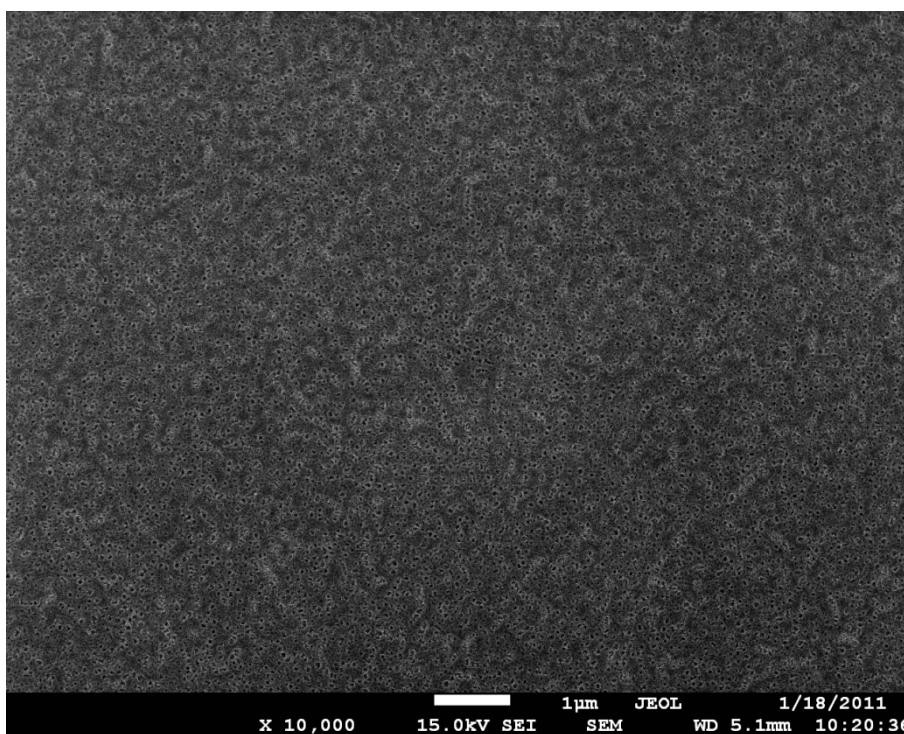


Selective on Site Separation and Detection of Molecules in Diluted Solution with Super-Hydrophobic Clusters of Plasmonic Nanoparticles

Francesco Gentile,^{*1,2} Maria Laura Coluccio,¹ Remo Proietti Zaccaria,² Marco Francardi,³ Gheorghe Cojoc,⁴ Gerardo Perozziello,¹ Raffaella Raimondo,¹ Patrizio Candeloro^a and Enzo Di Fabrizio^{3,1}

Supporting Information #1. Ultra high resolution SEM images for determining the average pore size and pore size distribution.

For estimating the pore size distribution in the porous substrates, we used ultra-high resolution SEM images. These images have a sufficient level of detail to allow a precise evaluation of the pore size distribution in the low meso-porous regime, that is, for pores larger than 2 nm, even without the need of adsorption/desorption isotherms. From these images, using image analysis algorithms used and described in⁴⁴, we derived the average pore size as $S=5$ nm. Notice that the pore size distribution may have tails that reach and surpass the 10 nm, and in fact the presented devices still harvest a reduced, and not null, amount of large Albumin molecules, as correctly indicated in the Results section. Here, we include additional SEM images of the sole pore substrates to further validate the pore size distribution.



¹ BioNEM, University Magna Graecia of Catanzaro - Catanzaro, 88100, Italy. E-mail:gentile@unicz.it

² Istituto Italiano di Tecnologia, Via Morego, 30 16163 Genova, Italy

³ King Abdullah University of Science and Technology, Thuwal 23955-6900, Kingdom of Saudi Arabia

⁴ Max Planck Institute of Molecular Cell Biology and Genetics, Pfotenhauerstrasse 108, 01307 Dresden, Germany

Figure S1.1

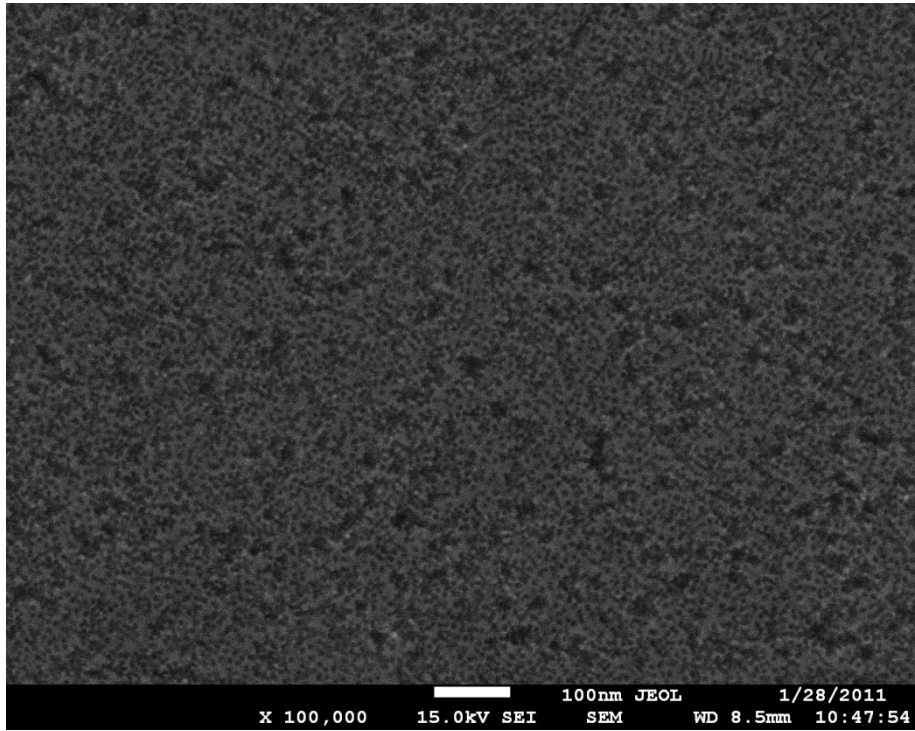


Figure S1.2

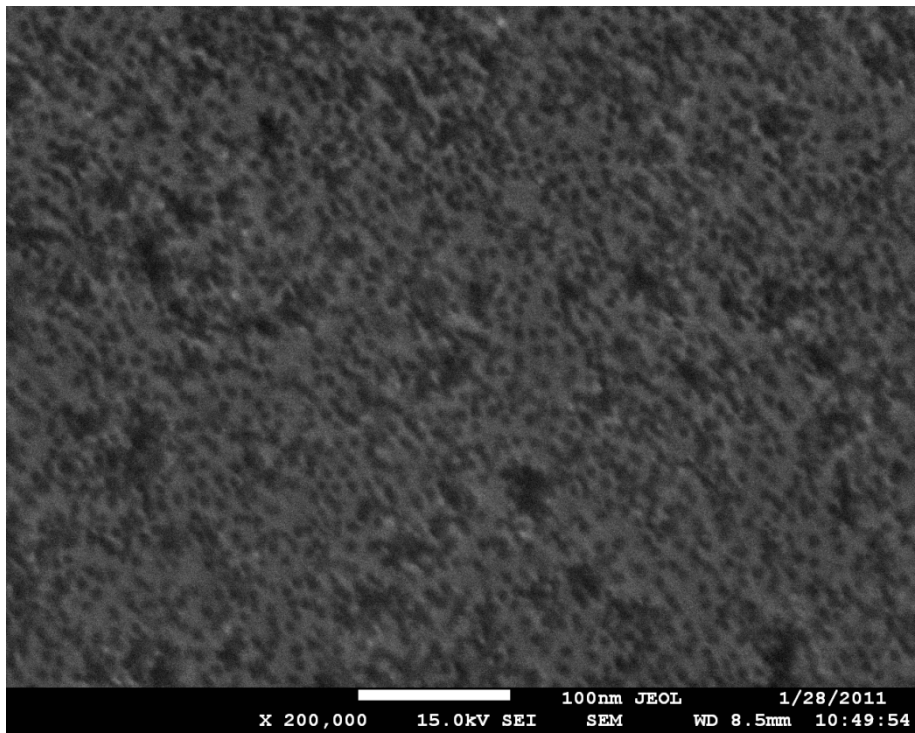


Figure S1.3

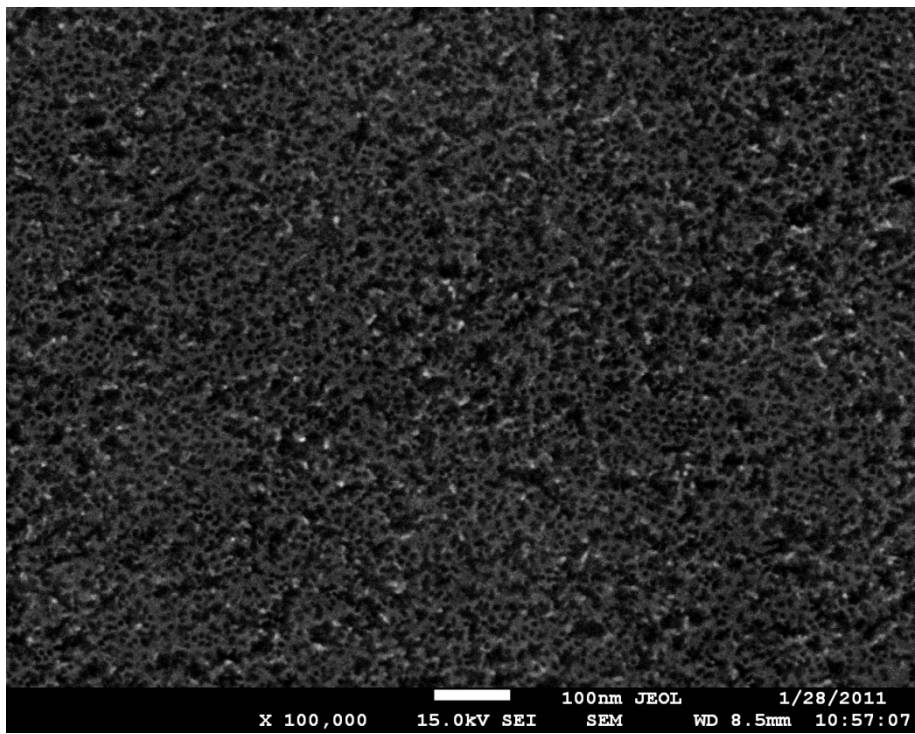


Figure S1.4

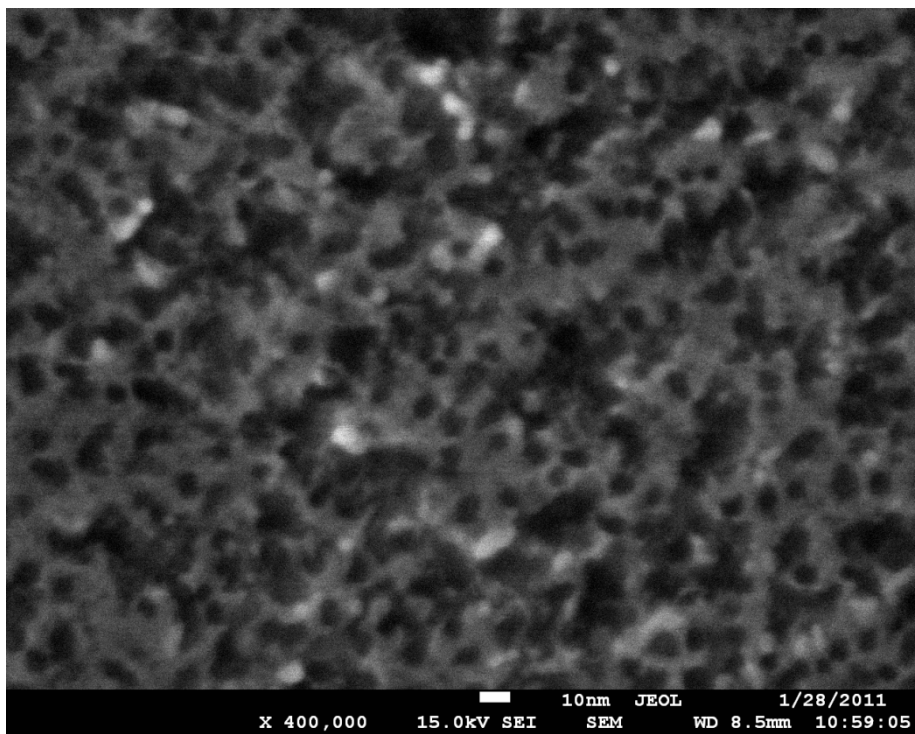


Figure S1.5

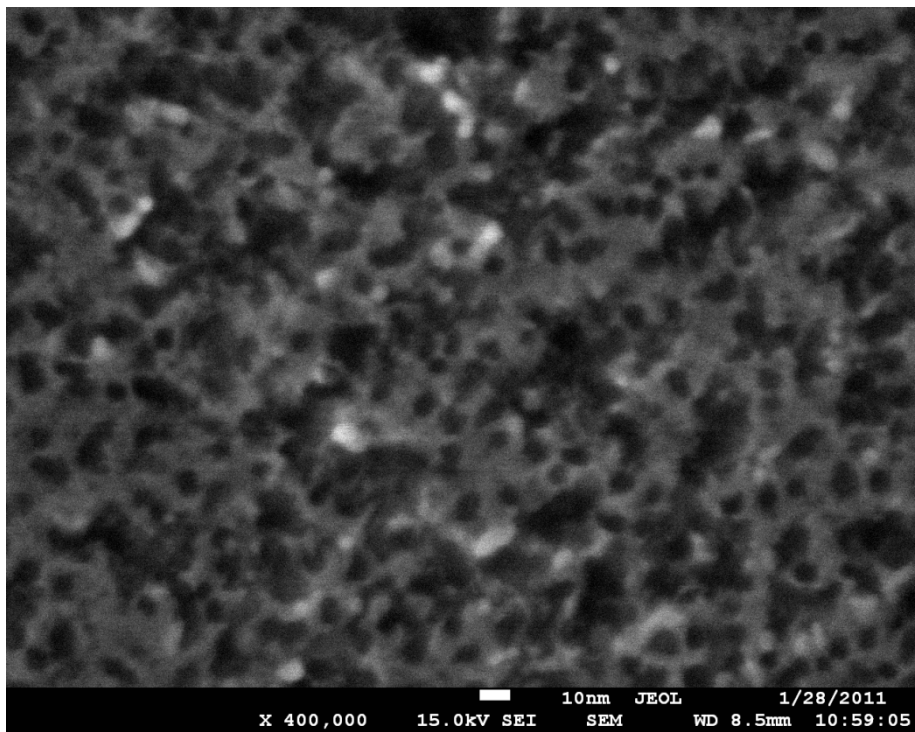


Figure S1.6

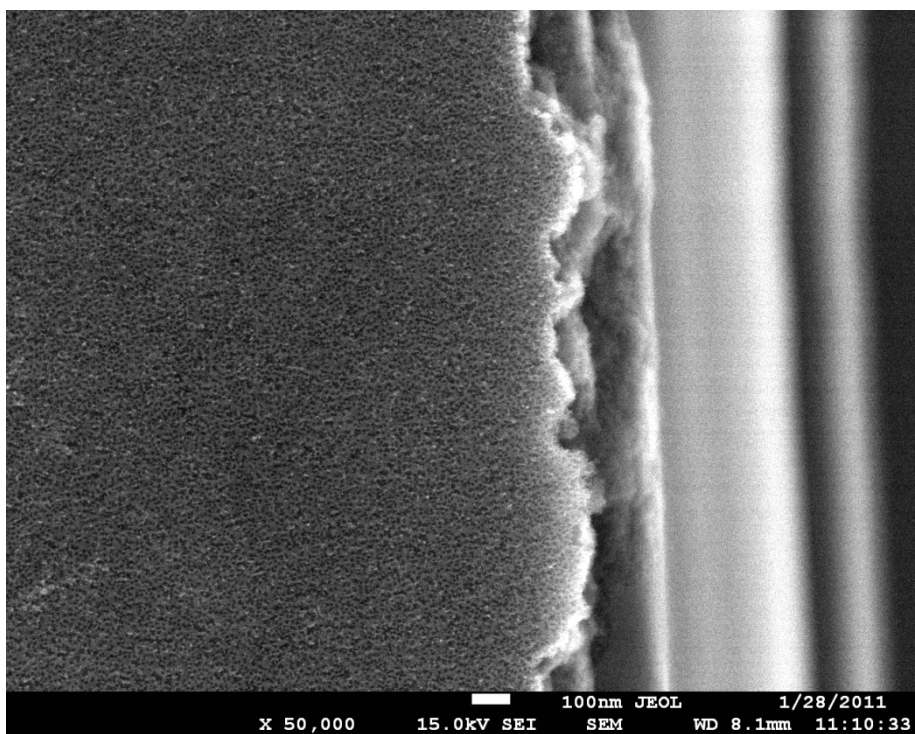


Figure S1.7

Supporting Information #2. Size and spatial distribution of the silver nanoparticles in the mesoporous silicon matrix.

The SEM images presented in the MS reveal that the silver nanoparticles accumulate, for the large majority, along the edges of the nano-pores, without occluding the pores. This effect can be ascribed to a non-uniform distribution of surface energy density that is larger on the pore borders (or edges) compared to that on bulk, flat silicon¹⁻⁴. The described increased energy density is responsible for the transport, sedimentation and growth the particles on the edges of the pores (for a thorough description of this mechanism, see the Appendix B in ⁵).

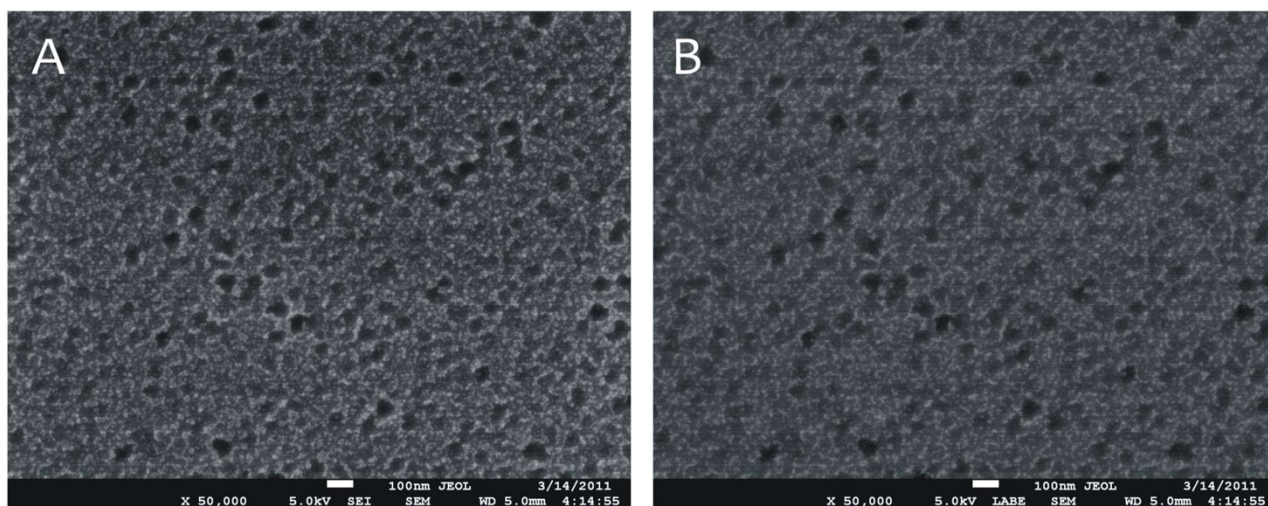


Figure S2.1

Here, we include additional SEM images that support these findings. The images show a bi-dimensional distribution of nanoparticles in a plane as to reproduce a complex network, where the average grain size is approximately 10 nm, and the cluster of particles resembles a hierarchical fractal structure (*Figure S2.1-2.2*). In the MS, mathematical modeling and computer simulations demonstrate that a similar configuration may increase the local EM field and the Raman signal of several orders of magnitude.

The cited increment takes place in a number of diverse hot spots randomly (and, on a larger micro scale, continuously) distributed on the surface of the pores ($z=0$). Assuming that small molecule are captured by the pores, it would be sufficient that those molecules would touch or intersect the $z=0$ plane in few points for guaranteeing matter-radiation interaction and SERS effects thereof (*Figure S2.3*).

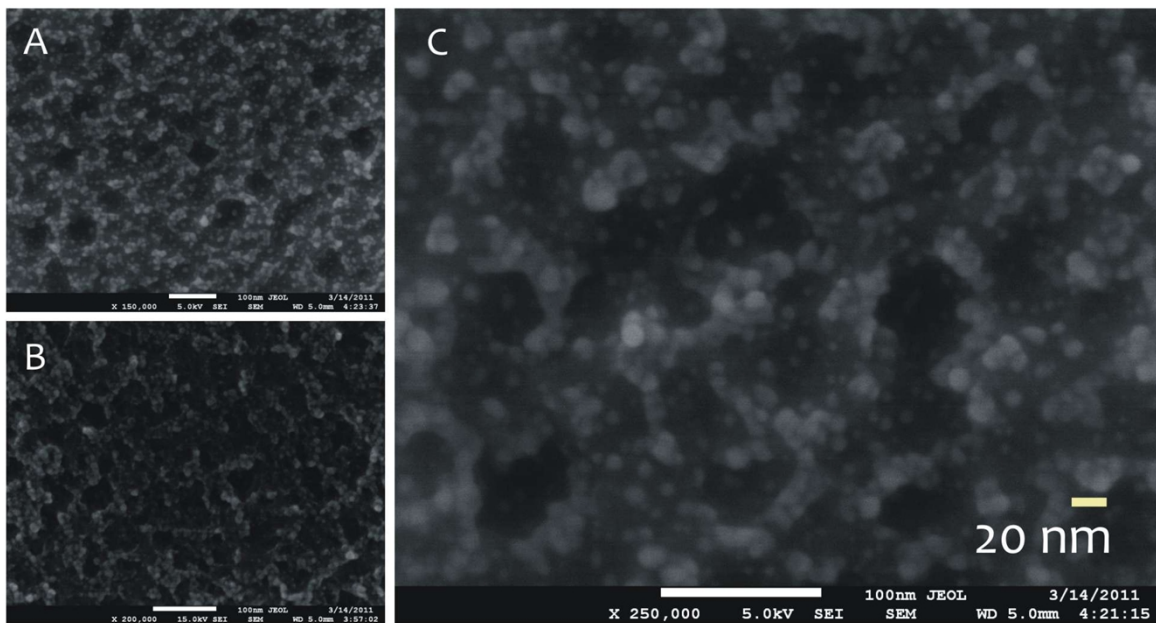


Figure S2.2

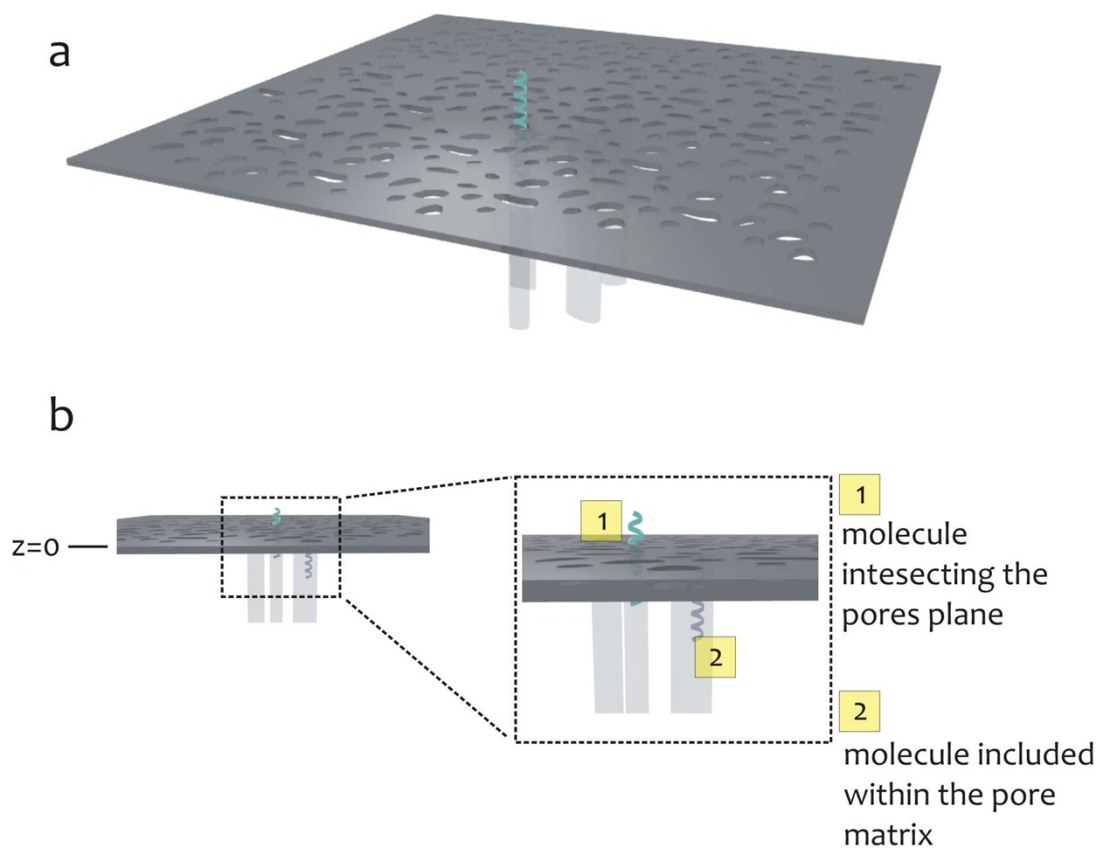


Figure S2.3

For certain growth configurations (far from equilibrium), particles in a network may be set apart, to form individual clusters, or isolated dimers of particles, with a particle size that may be larger than 10 nm, approaching and surpassing, in some cases, 20 nm (*Figure S2.4-S2.7*).

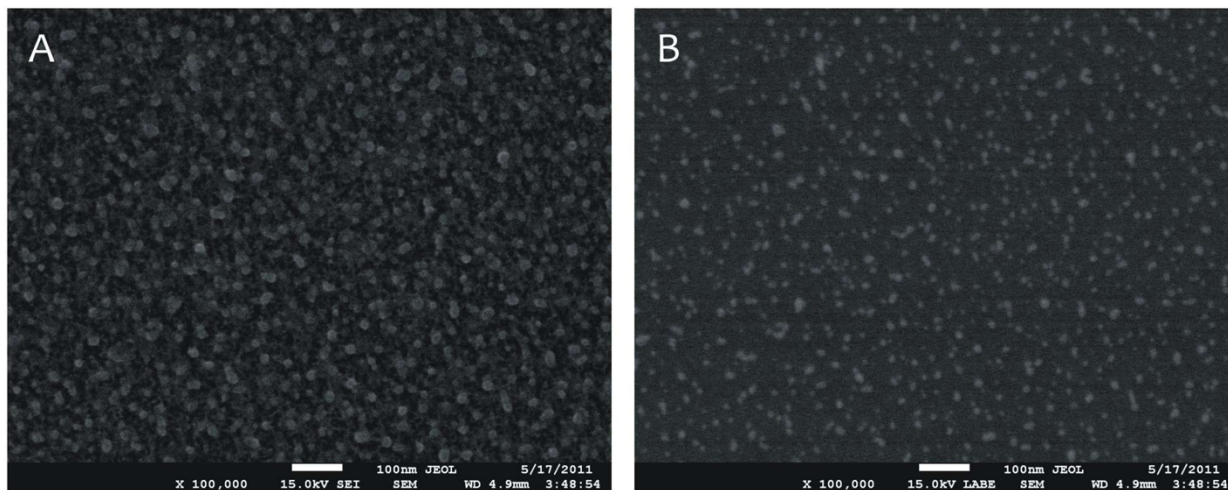


Figure S2.4

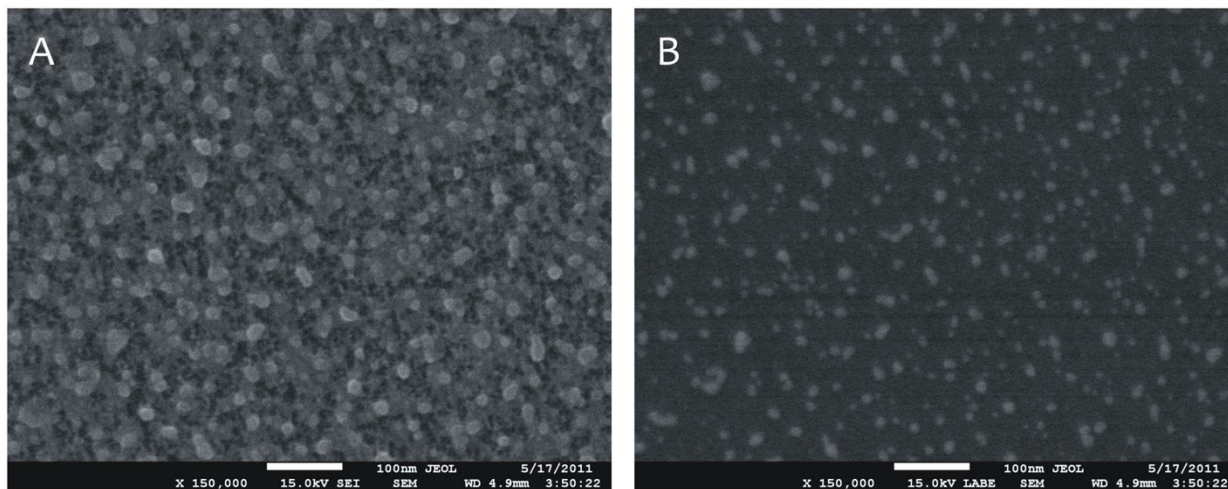


Figure S2.5

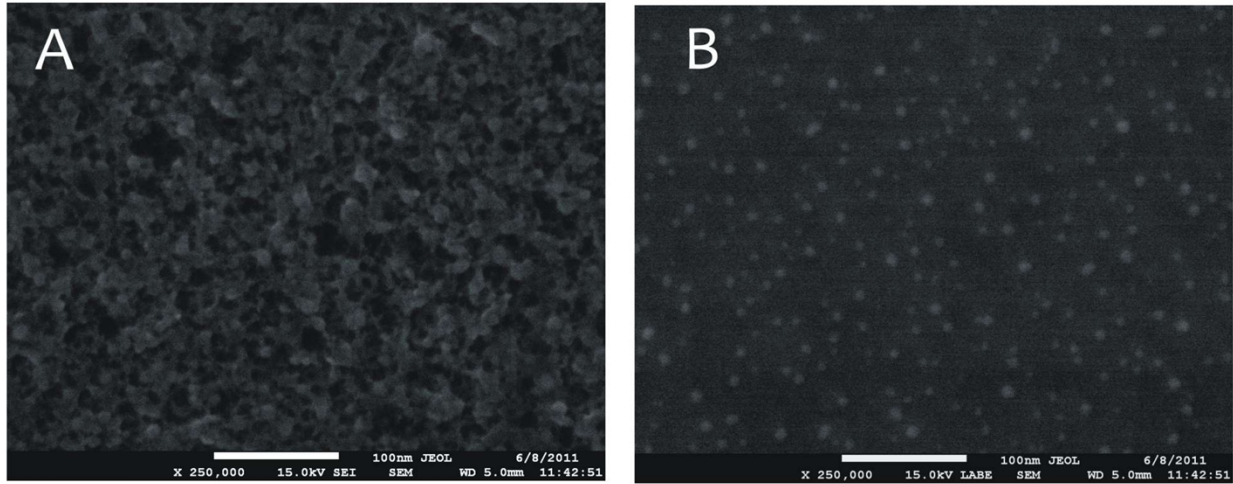


Figure S2.6

Notice that, even in this case (similarly to the general case of a multi-particles, self-similar configuration) a similar system of nano-particles may still generate giant EM fields, as described in ².

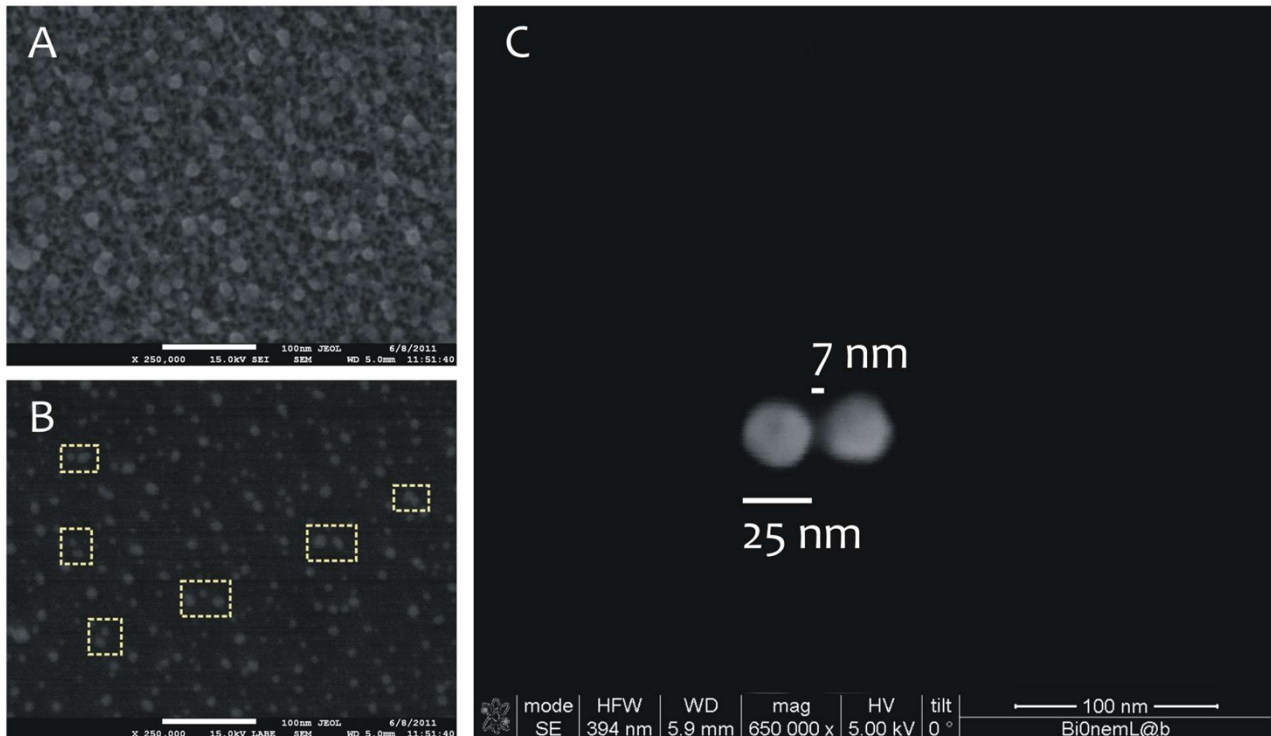


Figure S2.7

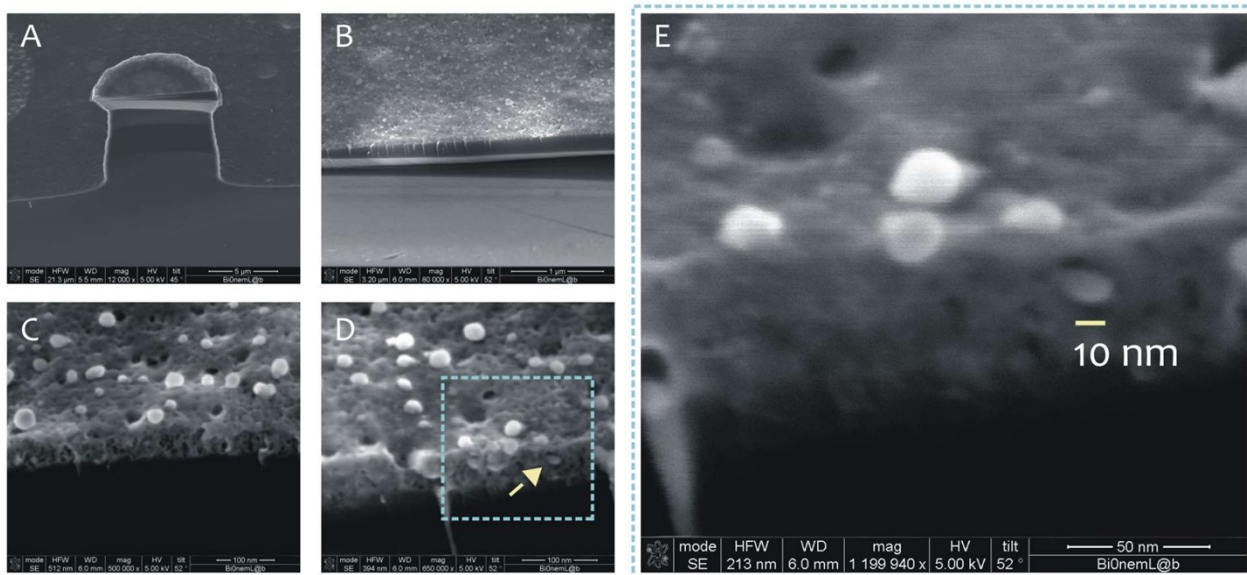


Figure S2.8

Finally, the cross-sectional SEM images in Figure S2.8 (where the conditions of growth and the growth itself has been exaggerated for illustrative purposes) indicate that, while some AgNPs are occasionally deposited in depth in the pore matrix, the majority of those nanoparticles are localized close to the $z=0$ surface, that is here defined as the interface between the original porous silicon sample and the upper air volume.

Supporting Information #3. Determining the relative content of Rhodamine and Albumin in a binary solution using a fitting procedure.

In this supporting information, we describe the procedure utilized to obtain the fit of a generic Raman spectrum of a binary mixture, and to derive, from this fit, the relative content of the species in the mixture.

Here, $n=2$ different chemical compounds were utilized to prepare the binary biological solution, that are

#1 - Rhodamine

#2 - Albumin

for each of these species, a Raman spectrum was acquired upon a SERS active substrate as described in the methods in the main text. Those spectra were therefore normalized to 1 using the maximum peak intensity contained in the acquisition range, that is $f_{inf} < f < f_{sup}$ ($f_{inf}=1050 \text{ cm}^{-1}$, $f_{sup}=3500 \text{ cm}^{-1}$), we shall call the cited spectra, p_1 (Rhodamine) and p_2 (Albumin).

We did divide p_1 and p_2 into $m=20$ non equally spaced intervals (being any interval limited by the following lower and upper bounds, 1050, 1500, 1750, 2000, 2100, 2250, 2300, 2500, 2750, 2800, 2900, 2950, 3000, 3050, 3100, 3150, 3200, 3250, 3350, 3500 cm^{-1}), to obtain a finite subset of $l=2 \times m$ linearly independent spectra, $\mathbf{s} = s_{11}, \dots, s_{1m}, s_{21}, \dots, s_{2m}$, where \mathbf{s} is a basis for the lattice of different possible combinations of p_1, \dots, p_2 . That is equivalent to say: every mixture containing, in different ratios, the species p_1, \dots, p_2 , produces a Raman spectrum s_M that can be fitted by the function

$$Y(f) = \sum_{i,j}^{n,m} x_{ij} s_{ij}(f) \quad (1)$$

where the index i runs through the number of species n ($i=1, \dots, n$), while j runs through the

number of intervals m ($j=1,\dots,m$). In (1), the coefficients x_{ij} are found as the best combination that minimizes the sum of the squares of deviations of Y from the experimental values s_M . From these, the functions, or weights, ξ_i

$$\xi_i = \int_{f_{inf}}^{f_{sup}} \left(\sum_{j=1}^m x_{ij} s_{ij}(f) \right) df / \int_{f_{inf}}^{f_{sup}} Y(f) df \quad (2)$$

may be derived, that indicate the mass fraction of the component i to the total solution. And thus, the larger ξ_i , the major the content of the peptide i in the mixture. Notice that the sum of the functions ξ_i over all the peptides m is one. In the right hand side of equation (2), the quantity

$$\Sigma_i = \sum_{j=1}^m x_{ij} s_{ij}(f) \quad (3)$$

represents the Raman spectrum of the i^{th} peptide contained in the solution, as derived from the fitting procedure. The goodness of fit metrics was verified by two parameters, and namely (i) the chi square statistics, χ^2 , and (ii) the coefficient of determination, r^2 .

Supporting Information #4. Verification of the small to large molecular weight separation abilities of the substrates, using UV-VIS spectroscopy techniques.

We report here further experiments to demonstrate independently the harvesting and selectivity capabilities of the presented meso-porous devices and substantiate the claims of the paper. We prepared solutions of (i) Rhodamine in D.I. water, (ii) Albumin in D.I. water, and (iii) a mixture of Rhodamine and Albumin in D.I. water in different concentrations ranging from 10^{-6} (that are, concentrated solutions) to 10^{-12} M (that are, diluted solutions). Therefore, we incubated the porous devices with the described solutions for 60 h. Consequently, we verified the release of molecules over time using UV-VIS spectroscopy techniques (spectrophotometer UV/Vis - LAMBDA 25 UV/Vis PerkinElmer), after standard calibration procedures of the samples.

The fluorescence emission spectrum of Rhodamine ranges from 555 to 585 nm with a maximum at 566 nm. The fluorescence emission spectrum of Albumin ranges from 240 to 320 nm with a maximum at 280 nm.

The results demonstrate that the samples previously loaded with Rhodamine (i) show an effective release over time, differently from Rhodamine (ii), the samples incubated with the solutions containing Albumin do not show an appreciable release at any time. Finally, in line with the described results, the samples incubated with the Rhodamine and Albumin mixture (iii) reveal a release curve that resembles, to a large extent, that of Rhodamine alone (Figure S4.1).

The described results would confirm the ability of the devices to separate and select the low molecular weight content of a mixture, where the cut off size can be conveniently controlled on changing the pore size of the meso-porous film.

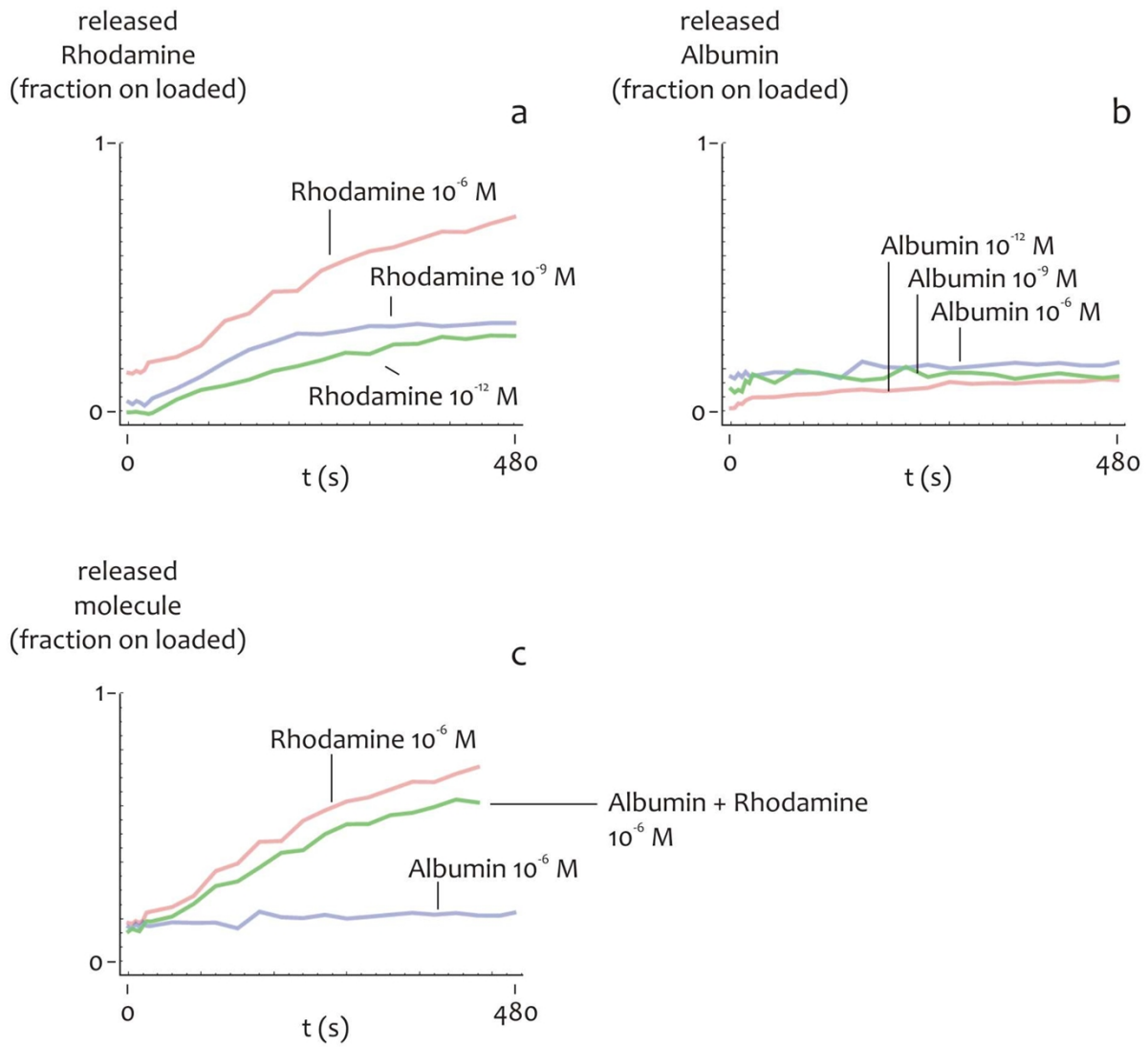


Figure S4.1